CuO-Decorated ZnO Nanotube-based Sensor for Detecting CO Gas: A First-Principles Study

Somayeh Tohidi
Tabriz University: University of Tabriz
Tavakkol Tohidi (ttouhidi@gmail.com)
Nuclear Science and Technology Research Institute https://orcid.org/0000-0001-8749-1401
Parvin Hamdi Mohammadabad
Azad University: Islamic Azad University

Research Article

Keywords: Nanotube, Zinc oxide, DFT, gas sensor, Electrical conductivity

Posted Date: April 29th, 2021

DOI: https://doi.org/10.21203/rs.3.rs-427186/v1

Abstract

Understanding the effect of decorating of copper oxide (CuO) on Carbon monoxide (CO) adsorption at zinc oxide nanotube is crucial for designing a high performance CO gas sensor. In this work, CO sensing properties of copper oxide-decorated zinc oxide (CuO-ZnO) nanotube is studied theoretically by employing first-principles density functional theory for the first time. The stability, adsorption mechanism, density of states, and change in electrical conductivity are studied. The results of calculating the adsorption energy show strong chemical adsorption of CO on CuO-ZnO nanotubes. The adsorption energy of CO on CuO-ZnO nanotube is calculated as 7.5 times higher than that on ZnO nanotube. The results of the Mulliken charge analysis reveal that electron transfer occurs from CO molecules to CuO-ZnO nanotubes. Additionally, the electrical conductivity of CuO-ZnO nanotubes significantly changes after adsorption of CO at room temperature. According to these studies, CuO-ZnO nanotube sensors can be used for the detection of CO gas. The results are in excellent agreement with the reported experimental results.

1. Introduction

Carbon monoxide (CO) is a highly toxic, colorless, odorless and tasteless gas. CO is a byproduct of the incomplete burning of fossil fuels with insufficient oxygen [1]. Exposure to a low concentration of CO (500 ppm) would lead to symptoms such as headache, dizziness, and nausea, whereas exposure to a higher concentration of more than 1500 ppm can result in death in most animate beings [2]. Therefore, CO gas detection is of great importance. Recently, various nanostructures have attracted extensive attention to develop sensing devices because of their high surface/volume ratio, good sensing performance, low-cost, and facility of miniaturization [3–14].

Zinc oxide (ZnO) is one of the most common nanostructures that has been extensively used in gas sensing devices due to its characteristics, such as superior electrical properties, chemical stability, and high electron mobility [15]. ZnO nanostructure has been reported to detect many hazardous gases, such as F2, NO2, NO, H_2S, CO_2, CO, triethylamine, ethanol, acetone, and chlorobenzene [16–22]. Nevertheless, pristine ZnO-based gas sensors had a weak interaction with different gas molecules. To solve this problem, some methods have been presented, including doping or decorating of impurity atoms, chemical functionalization, and introducing structural defects [23–25]. For example, Wei et al. [26] reported Pd-doped ZnO nanofibers with faster response and improved CO sensing. Lingmin et al. [27] showed that Al-doped ZnO nanovases exhibit four times better CO sensing response compared to the un-doped system.

However, it is a controversial issue to know how the doping or decorating of impurities changes the response of ZnO nanostructures in detecting CO. First-principles density functional theory (DFT) is a strong technique that can be utilized to explain the experimental results at the molecular level. For CO detection, a gas-solid interaction is needed to change the electronic properties on the ZnO surface through charge transfer mechanism. An et al. [28] studied the adsorption of gas molecules on ZnO (6,0) single-walled nanotubes with and without oxygen vacancy. They showed that CO molecules form C – Zn

bonds with a length of 2.67Å, an adsorption energy of -0.22 eV and 0.18 $|e|$ charge transfer from the CO molecules to the nanotube. Aslanzadeh [29] showed that V- and Cr-doped $Zn_{12}O_{12}$ nanoclusters have highly improved sensitivity to CO. Hadipour et al. [30] studied the adsorption of CO molecules on Al-doped ZnO nanoclusters. They found that C-Al bonds (1.95 Å and 2.07 Å) are formed with a remarkable decrease in the band gap energy. Here, for the first time, we perform a DFT study to investigate the adsorption of CO gas on CuO-decorated ZnO nanotubes. Moreover, different adsorption configurations of CO gas are considered. Charge transfer occurs between CO molecules and ZnO nanotube surface because of chemical adsorption.

2. Simulation And Calculation

These calculations were carried out based on the density functional theory by using a plane-wave base set and pseudopotential implemented in the Quantum Espresso package [31]. The generalized gradient approximation (GGA) in the Perdew-Burke-Ernzerhof (PBE) form was employed to compute the exchange-correlation energy-density functional. According to the Monkhorst-pack scheme, the Brillouin zone was sampled by 8 × 1 × 1 k-point mesh for structural optimization. An energy cut-off of 80 Ry was utilized for the plane wave expansion to solve the Kohn–Sham equations. In all calculations, atomic positions were optimized until the convergence threshold on total energy (a.u) and forces (a.u) were 10^{-8} and 10^{-7}, respectively. Moreover, the convergence threshold (conv-thr) for selfconsistency was 10^{-10}. An armchair single-walled nanotube structure was considered with 30 zinc atoms and 30 oxygen atoms.

CO and CuO get close to ZnO in various positions with respect to the symmetry axis parallel and perpendicular to the plane in four states at top positions of zinc-oxygen atoms (Top or T_1-Type and T_2-Type), the zinc-oxygen bond bisector perpendicular (Bridge or B-Type) and the center of the hexagonal structure of ZnO nanotube (Hollow or H-Type) as shown in Figs. 1A and 1B. Therefore, the 16 possible configurations with CO close to ZnO nanotube were: a_1T_1, a_2T_1, a_3T_1, a_4T_1, a_1B, a_2B, a_3B, a_4B, a_1T_2, a_2T_2, a_3T_2, a_4T_2, a_1H, a_2H, a_3H, and a_4H. The 16 possible configurations with CuO close to ZnO nanotube were: b_1T_1, b_2T_1, b_3T_1, b_4T_1, b_1B, b_2B, b_3B, b_4B, b_1T_2, b_2T_2, b_3T_2, b_4T_2, b_1H, b_2H, b_3H, and b_4H. Next, the most optimal configuration was chosen.

CO gets close to CuO-ZnO nanotube in three states with the symmetry axis parallel and perpendicular to the plane in three states according to Fig. 1C. 3; possible configurations in this case were: C_1T, C_2T, and C_3T, so the most optimal configuration could be investigated (Fig. 1C).

The binding energy (E_{bind}) of all possible configurations of adsorption of CO and CuO molecules on ZnO nanotube was calculated by:

$$E_{bind} = E_{total} - (E_{(Zno\ nanotube)} + E_{molecule}) \quad (1)$$

where E_{total} is the total energy of CuO adsorbed on ZnO nanotube, $E_{(Zno\ nanotube)}$ is the total energy of the ZnO nanotube, and $E_{molecule}$ is the total energy of free CO or CuO molecules. Moreover, to find the binding

energy, E_{bind}, between CO and CuO-ZnO nanotube structure (CO/CuO-ZnO nanotube), the following equation was used:

$$E_{bind} = E_{total} - (E_{(CuO-Zno\ nanotube)} + E_{CO}) \quad (2)$$

where E_{total} is the total energy of the CuO-ZnO nanotube structure interacting with CO gas, $E_{CuO-ZnO\ nanotube}$ is the total energy of the CuO-ZnO nanotube structure, and E_{CO} is the total energy of free CO molecules. The most stable configuration corresponds to a binding energy with the largest negative value.

Charge transfer is calculated from Mulliken charge analysis as follows:

$$Q_t = Q_{(Adsorbed\ molecule)} - Q_{(Isolateded\ molecule)} \quad (3)$$

In addition, the recovery time of (CO molecules from) ZnO and CuO-ZnO nanotube structures can be obtained as follows [32]:

$$\tau = \vartheta_0^{-1} exp\left(\frac{-E_{ads}}{kT}\right) \quad (4)$$

where k and T are the Boltzmann's constant (8.62×10^{-5} eV K^{-1}) and temperature, respectively; ϑ_0 denotes the attempt frequency ($\vartheta_0 = 10^{12} s^{-1}$).

3. Results And Discussion

3.1. CO adsorption on ZnO nanotube

In this section, the adsorption of CO on ZnO nanotube is investigated. In these calculations,, first, the structures of CO and pure ZnO nanotubes were optimized. Then, the C—O bond length in carbon monoxide and Zn—O bond length in ZnO nanotube were calculated as 1.12 and 1.87 Å, respectively. These bond lengths are comparable to those obtained in the previously reported results [33–36].

The binding energy of all 16 configurations of adsorption of CO on ZnO nanotube and C-O bond length (d_{C-O}) were calculated (Table 1). The calculated binding energies have negative values in all configurations. According to the results, the a_3T_2 configuration is the most optimal state after adsorption. The calculated binding energy at the most optimal position (a_3T_2) is equal to -0.63 eV.

This adsorption energy is in accordance with earlier reports about the adsorption of CO/ZnO nanotube [28], H_2 and O_2/ZnO nanotube [35], HCHO and O_2/ZnO nanotube [33].

The optimal structure is shown in Fig. 2A. The Mulliken charge analysis was used to compute the charge transfer between CO and the surface of ZnO nanotube. The results showed that after the adsorption of

CO on ZnO, their charges become more positive and negative, respectively. Thus, during the adsorption process, CO behaves as an electron donor and ZnO as an electron acceptor.

The net charge transfer from CO to ZnO was calculated as 0.019 electrons and the small charge transfer between gas molecules and ZnO nanotube is similar to other reports [33, 35].

The recovery time at room temperature was 3.79×10^{-2} s. According to Eq. (4), for greater values of E_{bind}, the recovery time increases. This reveals that the greater negative values of E_{bind} means stronger interaction between the CO molecules and ZnO nanotubes, which increases the recovery time.

Table 1

Calculated values of adsorption energies (E_{bind}) and the bond length (d) of CO in CO/ZnO nanotube.

Sites	E_{bind} (eV)	d_{C-O} (Å)
a_1T_1	**-0.39**	1.11
a_1B	**-0.58**	1.14
a_1T_2	**-037**	1.15
a_1H	**-0.35**	1.14
a_2T_1	**-0.32**	1.12
a_2B	**-0.55**	1.16
a_2T_2	**-0.31**	1.11
a_2H	**-0.33**	1.15
a_3T_1	**-0.46**	1.15
a_3B	**-0.52**	1.13
a_3T_2	**-0.63**	1.17
a_3H	**-0.35**	1.14
a_4T_1	**-0.32**	1.11
a_4B	**-0.36**	1.13
a_4T_2	**-0.33**	1.15
a_4H	-0.49	1.14

The energy density of states was calculated before and after the adsorption of CO on ZnO nanotube and the curve is shown in Fig. 3B. No considerable change or evidence of hybridization between the CO molecules and ZnO nanotubes was observed by comparing the density of states of ZnO nanotube with that of CO/ZnO nanotubes near the Fermi level. This result is completely in agreement with the obtained weak adsorption energy and small charge transfer. Therefore, it can be concluded that the electronic properties of the ZnO nanotubes remain unchanged after adsorbing CO molecules.

3.1. Adsorption of CuO on ZnO nanotubes

Calculations were performed for all possible adsorption configurations. In these calculations, first, the structures of CuO was optimized. Then, the Cu—O bond length in copper oxide was calculated as 1.72 Å which is agreement with other reported Cu—O bond length [37, 38].The adsorption of CuO molecules on ZnO nanotubes was investigated. The results of adsorption energy of all 16 configurations of CuO molecules on ZnO nanotubes are shown in Table 1.

The results indicate the adsorption of CuO on ZnO nanotube and the formation of CuO-decorated ZnO (CuO-ZnO) nanotube. The configuration b_1T_1 was the most optimal state for the CuO-ZnO nanotube as shown in Fig. 2. In this structure, the bond lengths of O—Zn and Cu—O are 2.32 and 1.70 Å, respectively. The net charge transfer from ZnO nanotube to CuO molecule was calculated as 0.117 electrons.

Table 2

Calculated values of adsorption energies (E_{bind}) and the bond length (d) of Cu-O in CuO-ZnO nanotube adsorption energies (E_{bind}) and the binding length (d) of Cu-O in CuO-ZnO nanotube

Sites	E_{bind} (eV)	d_{Cu-O} (Å)
b_1T_1	**-1.91**	1.72
b_1B	**-1.22**	1.69
b_1T_2	**-0.73**	1.72
b_1H	**-0.84**	1.72
b_2T_1	**-0.87**	1.68
b_2B	**-1.34**	1.72
b_2T_2	**-0.89**	1.69
b_2H	**-0.87**	1.69
b_3T_1	**-0.81**	1.66
b_3B	**-1.21**	1.69
b_3T_2	**-1.57**	1.77
b_3H	**-0.86**	1.73
b_4T_1	**-0.88**	1.68
b_4B	**-0.91**	1.72
b_4T_2	**-0.89**	1.68
b_4H	-0.87	1.69

The density of states of ZnO nanotube was calculated before and after adsorbing CuO in the most optimal configuration; the curves relative to Fermi level are plotted in Fig. 3A. As can be observed, the energy density of states for CuO-ZnO nanotube is different from that for ZnO nanotube, particularly around the Fermi level, indicating the proper adsorption of ZnO nanotube.

3.3. CO adsorption on CuO-ZnO nanotube

This section evaluates the mechanism of adsorption of CO on CuO-ZnO nanotube. The adsorption of CO on CuO-ZnO nanotube is investigated for three different configurations of C_1T, C_2T, and C_3T as shown in Fig. 1C. The binding energies for configurations C_1T, C_2T, and C_3T are equal to -4.76, -2.86, and − 1.98 eV, respectively. Figure 4A illustrates the optimal structure and the bond length for the adsorption of CO on CuO-ZnO nanotube (C_1T). The results show that the absorption of CuO on ZnO nanotube enhances the

capability of CuO-ZnO nanotube to detect CO gas. The net charge transfer from CO to CuO-ZnO nanotube was computed as 0.3189 electrons.

This results is in agreement with other reported results about the adsorption of O_2/Pt-ZnO nanotube [35], O_2/Pd-ZnO and HCHO/O_2/Pd-ZnO nanotube [33], H_2@ZnO-NT:V_O [34], CO/Al-ZnO [39], CO/Al- and Cu-ZnO [40].

The recovery time of CuO-ZnO nanotube at room temperature was calculated as 8.63×10^{17} s. From the results of recovery time, a larger negative value for E_{bind} means longer desorption time of CO gas molecules from the CuO-ZnO nanotube. Additionally, the strong adsorption of CO on CuO-ZnO nanotube (i.e., with long recovery time and high adsorption energy) indicates that the CuO-ZnO nanotube slowly recovers to its original state

Figure 4B shows the changes in the energy density of states of CuO-ZnO nanotube computed after the adsorption of CO gas. The obtained results show the changes in charge distribution in the structure after the adsorption of CO. These changes indicate that the CuO-ZnO nanotube can adsorb CO gas, which is consistent with the results of the adsorption energy.

The electron orbital overlap of bonding atoms is illustrated in Fig. 4C. The obtained results indicate that the orbitals of CO atoms (carbon and oxygen) have a good overlap with the orbital of the oxygen atom in CuO.

According to our calculations, by the adsorption of CuO on ZnO nanotube, the capability of this structure for CO gas detection considerably increases as compared to ZnO nanotube, so this compound can be used in CO gas sensors. Our results are in good agreement with the reported experimental results [41–44]. This experimental studies have demonstrated that the sensing response to CO of the gas sensors using ZnO nanostructures could be enhanced by decorating of CuO.

3.4. Electrical conductivity of optimized configurations

In this section, the electrical conductivity (σ/τ) is calculated as a function of the chemical potential at room temperature (300 K) using Boltzmann Transport Properties (BoltzTrap) code [45]. The variations of electrical conductivity of the ZnO and CuO-ZnO nanotubes were computed before and after the adsorption of CO molecules in the range − 2 to 2 eV; the results are illustrated in Fig. 5 (a, b, and c). The variations of electrical conductivity in Fig. 5 show that the electrical conductivities of the ZnO and CuO-ZnO nanotubes before and after the adsorption of the CO molecules increase above the Fermi level. Changes in electrical conductivity is related to the changes in the resistivity of the system, which is a measurable quantity. According to these results, the electrical conductivity in CuO is due to the adsorption of CO by CuO-ZnO nanotube and better electron transfer by ZnO nanotube (according to the energy adsorption calculations). Furthermore, the results show that CuO-ZnO is much better than ZnO in CO detection.

4. Conclusion

The adsorption of CO gas on CuO-ZnO nanotube was theoretically investigated. The results illustrated that compared to pristine ZnO nanotube, CuO-decorated ZnO nanotube was more sensitive to CO molecules. Moreover, it was found that CO prefers to be adsorbed on CuO-ZnO nanotube with an excellent E_{bind} of − 4.76 eV. The density of states revealed the changes in the band gap and charge transfer, which influence the conductivity of the CuO-ZnO nanotube. It was also found that the electrical conductivity of CuO-ZnO nanotube varies in the range − 2 to 2 eV, which is more than twice the change in the conductivity due to the adsorption of CO on ZnO nanotube. This considerable change emphasizes the key role of electrostatic exchanges of CuO in CuO-ZnO nanotube. Therefore, the CuO-ZnO nanotube nanostructure can be used to detect CO by changing electrical conductivity properties.

5. Declarations

Ethics approval: This article does not contain any studies with human participants or animals performed by any of the authors.

Consent to participate: The authors declare the consent to participate.

Consent for publication: The authors declare the consent for publication.

Conflict of interest: The authors have no conflicts of interest to declare that are relevant to the content of this article.

Funding information: This research did not receive any specific grant from funding agencies in the public, commercial, or not-for-profit sectors.

Data availability and materials: N/A.

Code availability: N/A.

Authors' contribution: All authors designed the project; ST and TT did the calculations; all authors contributed to the writing of the manuscript.

6. References

1. Hoa ND et al (2014) Effective decoration of Pd nanoparticles on the surface of SnO2 nanowires for enhancement of CO gas-sensing performance. J Hazard Mater 265:124–132
2. Takeda H et al (2015) CO-sensing properties of a NASICON-based gas sensor attached with Pt mixed with Bi2O3 as a sensing electrode. Electrochim Acta 155:8–15
3. Beheshtian J et al (2013) Ammonia monitoring by carbon nitride nanotubes: a density functional study. Thin solid films 534:650–654

4. Dos Santos RB et al (2011) Effects of N doping on the electronic properties of a small carbon atomic chain with distinct s p 2 terminations: A first-principles study. Phys Rev B 84(7):075417
5. Samadizadeh M, Rastegar SF, Peyghan AA (2015) F−, Cl−, Li + and Na + adsorption on AlN nanotube surface: a DFT study. Physica E 69:75–80
6. Wang Y-Z, Li F-M (2016) Dynamical parametric instability of carbon nanotubes under axial harmonic excitation by nonlocal continuum theory. J Phys Chem Solids 95:19–23
7. Baei MT, Peyghan AA, Bagheri Z (2012) A computational study of AlN nanotube as an oxygen detector. Chin Chem Lett 23(8):965–968
8. Bandyopadhyay A, Paria S, Jana D (2018) Tetragonal graphene nanodot as carbon monoxide gas sensor and current rectification device. J Phys Chem Solids 123:172–182
9. Baei MT et al (2012) B-doping makes the carbon nanocones sensitive towards NO molecules. Phys Lett A 377(1–2):107–111
10. An S et al (2013) Enhanced ethanol sensing properties of multiple networked Au-doped In2O3 nanotube sensors. J Phys Chem Solids 74(7):979–984
11. Pashangpour M, Peyghan AA (2015) Adsorption of carbon monoxide on the pristine, B-and Al-doped C 3 N nanosheets. J Mol Model 21(5):1–7
12. Lu X et al (2018) Freeze drying-assisted synthesis of Pt@ reduced graphene oxide nanocomposites as excellent hydrogen sensor. J Phys Chem Solids 116:324–330
13. dos Santos RB et al (2012) Exploring hydrogenation and fluorination in curved 2D carbon systems: a density functional theory study on corannulene. The Journal of Physical Chemistry A 116(36):9080–9087
14. Eslami M, Peyghan AA (2015) DNA nucleobase interaction with graphene like BC3 nano-sheet based on density functional theory calculations. Thin Solid Films 589:52–56
15. Sahay P (2005) Zinc oxide thin film gas sensor for detection of acetone. J Mater Sci 40(16):4383–4385
16. Peyghan AA, Rastegar SF, Bagheri Z (2015) Selective detection of F 2 in the presence of CO, N 2, O 2, and H 2 molecules using a ZnO nanocluster. Monatshefte für Chemie-Chemical Monthly 146(8):1233–1239
17. Gu C et al (2016) Chlorobenzene sensor based on Pt-decorated porous single-crystalline ZnO nanosheets. Sensors Actuators A: Physical 252:96–103
18. Wei A, Pan L, Huang W (2011) Recent progress in the ZnO nanostructure-based sensors. Materials Science Engineering: B 176(18):1409–1421
19. Hosseini Z, Mortezaali A (2015) Room temperature H2S gas sensor based on rather aligned ZnO nanorods with flower-like structures. Sens Actuators B 207:865–871
20. Jeong Y-J, Balamurugan C, Lee D-W (2016) Enhanced CO2 gas-sensing performance of ZnO nanopowder by La loaded during simple hydrothermal method. Sens Actuators B 229:288–296

21. Shohany BG, Motevalizadeh L, Abrishami ME (2018) Investigation of ZnO thin-film sensing properties for CO 2 detection: effect of Mn doping. Journal of Theoretical Applied Physics 12(3):219–225
22. Lim SK et al (2011) Preparation of ZnO nanorods by microemulsion synthesis and their application as a CO gas sensor. Sens Actuators B 160(1):94–98
23. Hjiri M et al (2014) Al-doped ZnO for highly sensitive CO gas sensors. Sens Actuators B 196:413–420
24. Galstyan V et al (2016) Reduced graphene oxide/ZnO nanocomposite for application in chemical gas sensors. RSC Adv 6(41):34225–34232
25. Dilonardo E et al (2016) Evaluation of gas-sensing properties of ZnO nanostructures electrochemically doped with Au nanophases. Beilstein journal of nanotechnology 7(1):22–31
26. Wei S, Yu Y, Zhou M (2010) CO gas sensing of Pd-doped ZnO nanofibers synthesized by electrospinning method. Mater Lett 64(21):2284–2286
27. Lingmin Y et al (2013) Gas sensing enhancement of aluminum-doped ZnO nanovase structure with many gas facile diffusivity paths. Applied surface science 265:108–113
28. An W, Wu X, Zeng XC (2008) Adsorption of O2, H2, CO, NH3, and NO2 on ZnO nanotube: a density functional theory study. J Phys Chem C 112(15):5747–5755
29. Aslanzadeh S (2016) Transition metal doped ZnO nanoclusters for carbon monoxide detection: DFT studies. J Mol Model 22(7):1–6
30. Hadipour NL, Ahmadi Peyghan A, Soleymanabadi H (2015) Theoretical study on the Al-doped ZnO nanoclusters for CO chemical sensors. J Phys Chem C 119(11):6398–6404
31. Giannozzi P et al (2009) QUANTUM ESPRESSO: a modular and open-source software project for quantum simulations of materials. Journal of physics: Condensed matter 21(39):395502
32. Nagarajan V, Chandiramouli R (2018) A novel approach for detection of NO2 and SO2 gas molecules using graphane nanosheet and nanotubes-A density functional application. Diam Relat Mater 85:53–62
33. Zhang Z, Sun W, Hamreh S (2020) A density functional theory study on the formaldehyde detection mechanism by Pd-decorated ZnO nanotube. J Phys Chem Solids 144:109511
34. Ali M, Tit N, Yamani ZH (2020) Role of defects and dopants in zinc oxide nanotubes for gas sensing and energy storage applications. Int J Energy Res 44(13):10926–10936
35. Li F, Asadi H (2020) DFT study of the effect of platinum on the H2 gas sensing performance of ZnO nanotube: Explaining the experimental observations. J Mol Liq 309:113139
36. Saputro AG et al (2017) Selectivity of CO and NO adsorption on ZnO (0002) surfaces: A DFT investigation. Appl Surf Sci 410:373–382
37. Asadi H, Vaezzadeh M (2017) Computational designing ultra-sensitive nano-composite based on boron doped and CuO decorated graphene to adsorb H2S and CO gaseous molecules. Materials Research Express 4(7):075039

38. Mohammadi-Manesh E, Vaezzadeh M, Saeidi M (2015) Cu-and CuO-decorated graphene as a nanosensor for H2S detection at room temperature. Surf Sci 636:36–41
39. Nguyen D et al (2020) Unraveling the effect of Al doping on CO adsorption at ZnO (101 [combining macron] 0). RSC Advances 10(67):40663–40672
40. Maarouf M, Al-Sunaidi A (2020) Investigating the chemisorption of CO and CO2 on Al-and Cu-doped ZnO nanowires by density-functional calculations. Comput Theor Chem 1175:112728
41. Huang J et al (2013) Preparation of porous flower-like CuO/ZnO nanostructures and analysis of their gas-sensing property. J Alloys Compd 575:115–122
42. Jung S-J, Yanagida H (1996) The characterization of a CuO/ZnO heterocontact-type gas sensor having selectivity for CO gas. Sens Actuators B 37(1–2):55–60
43. Simon Q et al (2012) CuO/ZnO Nanocomposite Gas Sensors Developed by a Plasma-Assisted Route. ChemPhysChem 13(9):2342–2348
44. Wu N et al (2005) Porous CuO–ZnO nanocomposite for sensing electrode of high-temperature CO solid-state electrochemical sensor. Nanotechnology 16(12):2878
45. Madsen GK, Singh DJ (2006) BoltzTraP. A code for calculating band-structure dependent quantities. Comput Phys Commun 175(1):67–71

Figures

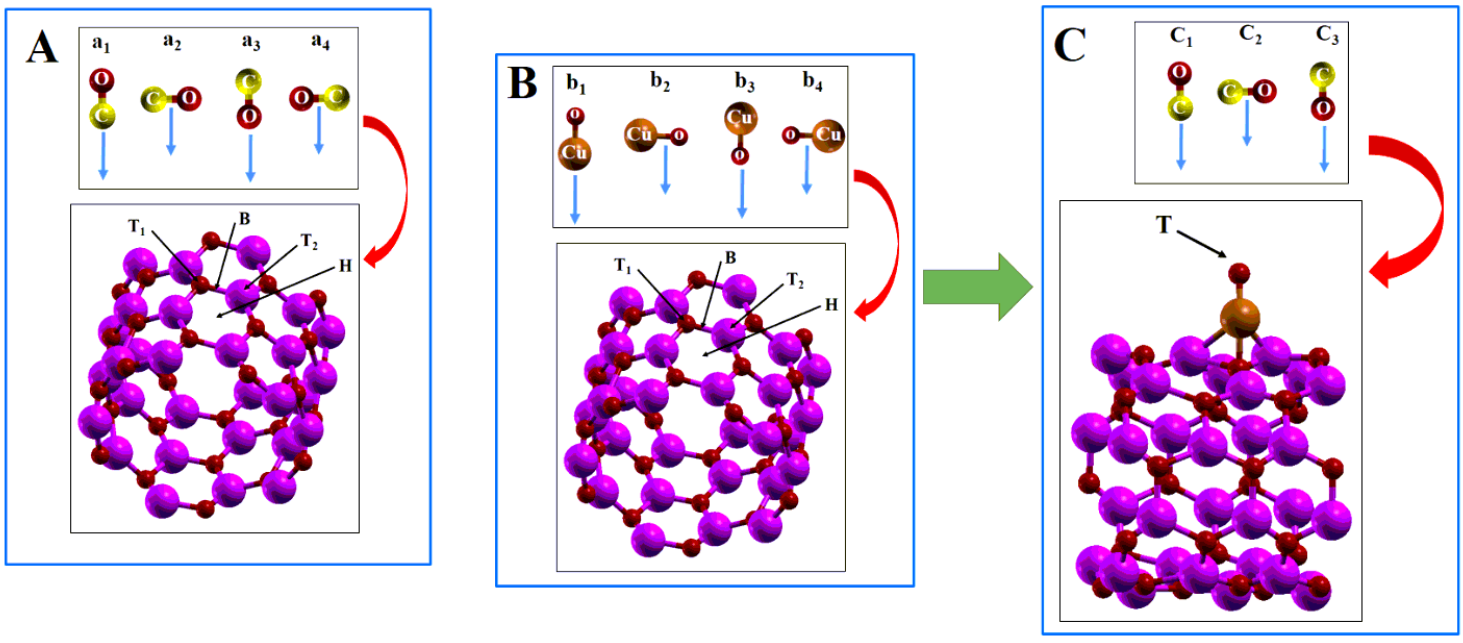

Figure 1

(A) Four different orientations of CO getting close to four positions to be adsorbed on ZnO nanotube, (B) four different orientations for Cu getting close to four positions to be adsorbed on ZnO nanotube, and (C) three different orientations for CO getting close to CuO-ZnO nanotube.

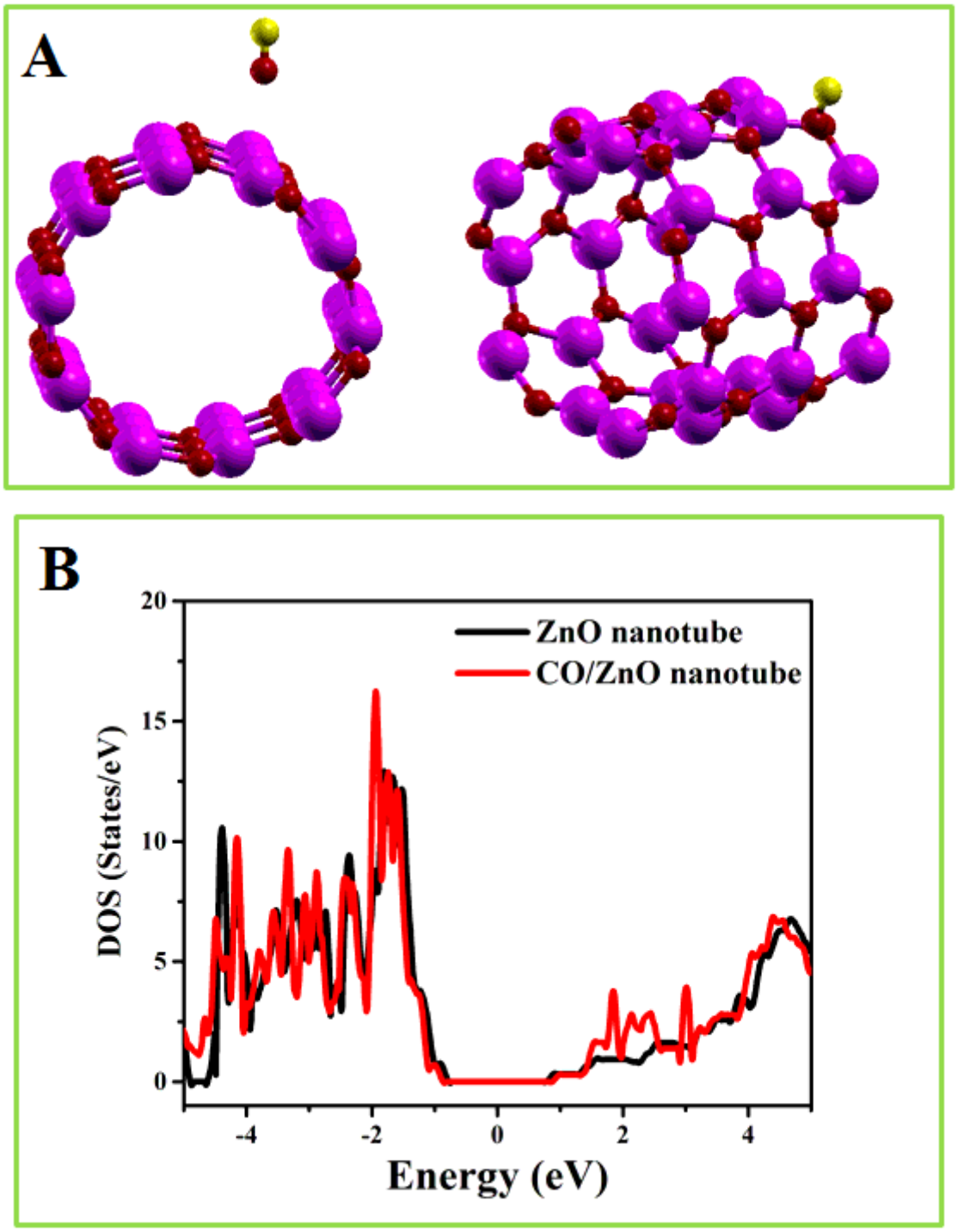

Figure 2

(A) Optimized configuration of CO/ZnO nanotube (a3T2), (B) calculated DOS for ZnO nanotubes (black line), and CO/ZnO nanotube structures for the a3T2 configuration (red line).

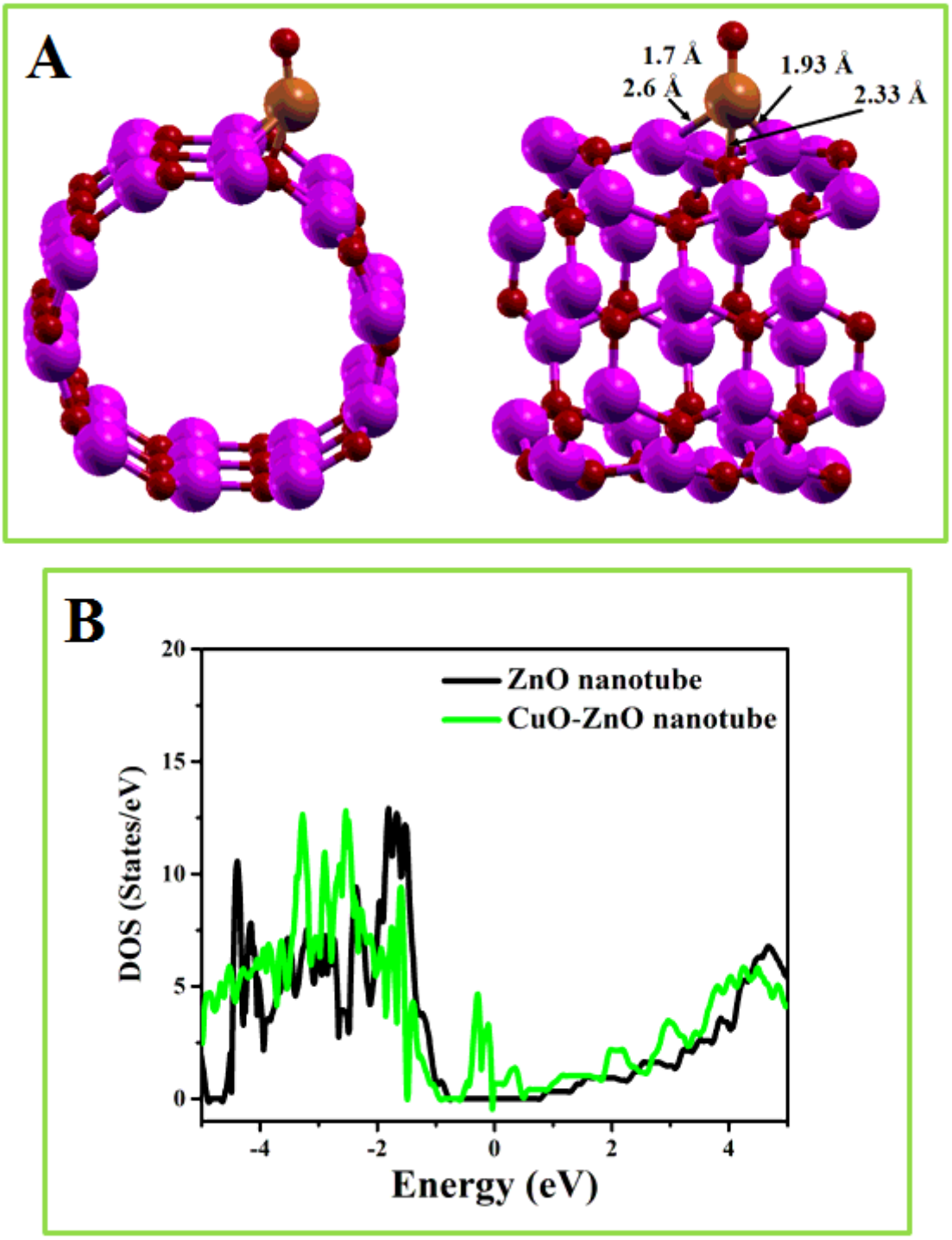

Figure 3

(A) Optimized configuration of CuO-ZnO nanotube (b1T1), (B) calculated DOS for ZnO nanotube (black line), and CuO-ZnO nanotube structures for the b1T1 configuration (green line).

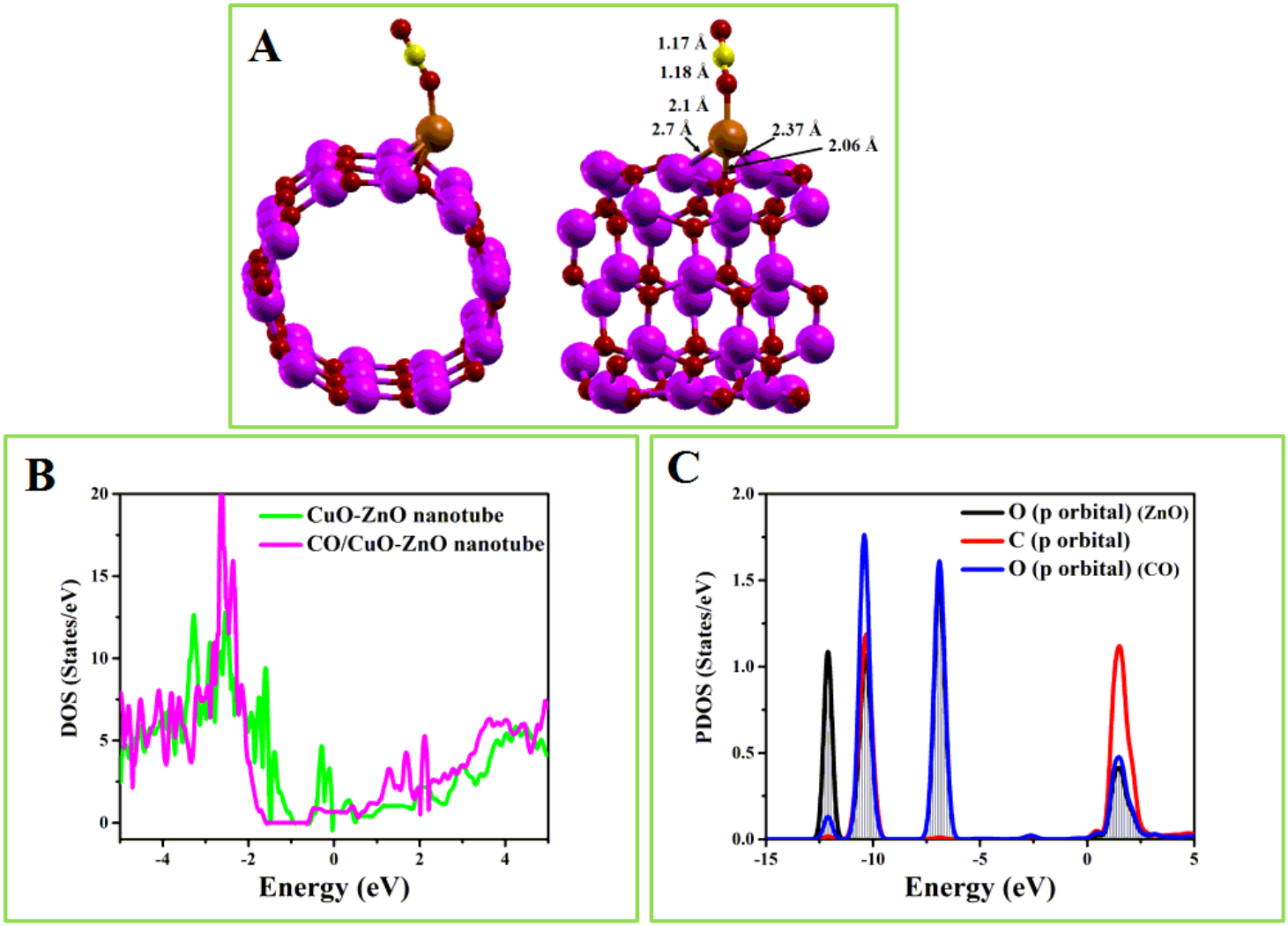

Figure 4

(A) Optimized configuration of CO/CuO-ZnO nanotube (C1T), (B) calculated DOS for CuO-ZnO nanotube (green line), and CO/CuO-ZnO nanotube structures for the C1T configuration (pink line).

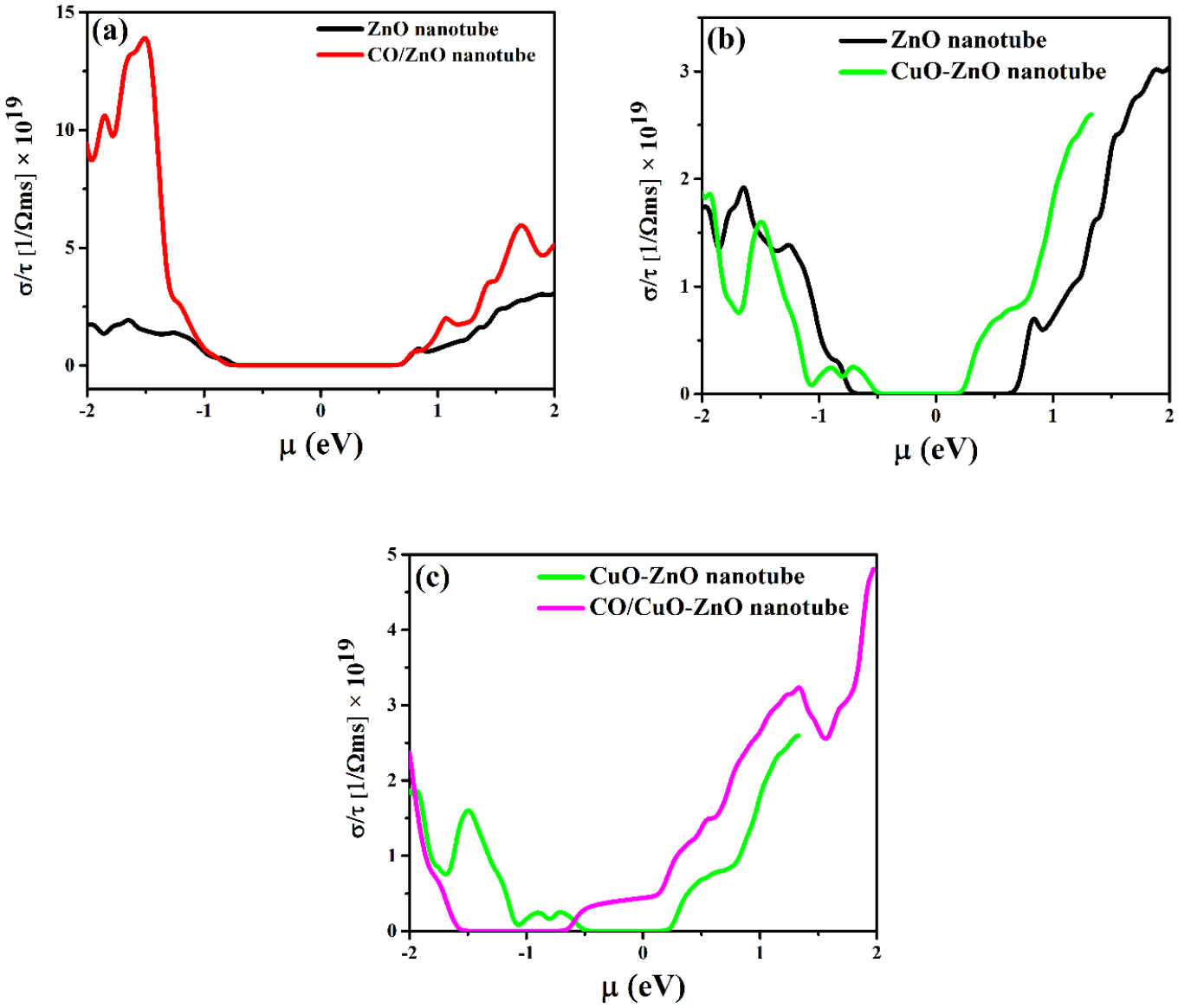

Figure 5

Electrical conductance per relaxation time versus chemical potential at room temperature for ZnO nanotube (black line), CO/ZnO nanotube structures for the a3T2 configuration (red line), CuO-ZnO nanotube structures for the b1T1 configuration (green line), and CO/CuO-ZnO nanotube structures for the C1T configuration (pink line).